

# Surface alteration of pentlandite and spectroscopic evidence for secondary violarite formation

S. RICHARDSON

Department of Geological Sciences, Aston University, Birmingham B4 7ET

AND

D. J. VAUGHAN

Department of Geology, The University, Manchester M13 9PL

## Abstract

Synthetic pentlandite surfaces were subjected to oxidation by a range of inorganic oxidants, and the resultant alteration of the surface studied by a range of surface-sensitive spectroscopic techniques. The oxidants used were air during heating to relatively low temperatures (150°C), steam, ammonium hydroxide, hydrogen peroxide, and sulphuric acid. Electrochemical oxidation was also undertaken. X-ray photoelectron spectroscopy (XPS), Auger electron spectroscopy (AES), conversion electron Mössbauer spectroscopy (CEMS), and spectral reflectance measurements were used to characterize the surface compositions. New data for the binding energies of core electrons in pentlandite and violarite, based on the fitted XPS spectra, are proposed. For pentlandite and violarite respectively, values of 707.3 eV and 708.4 eV for the Fe  $2p^{3/2}$ , 853.0 eV and 853.2 eV for the Ni  $2p^{3/2}$ , and 161.2 eV for the S  $2p$  in both sulphides, were obtained. After oxidation the pentlandite surfaces indicated nickel enrichment in the subsurface, with the formation of violarite. The immediate oxidized surface, of approximately 10 Å thickness, indicated a range of iron oxides and hydroxides (Fe<sub>3</sub>O<sub>4</sub>, Fe<sub>2</sub>O<sub>3</sub> and FeOOH, with possible Fe<sub>1-x</sub>O and Fe(OH)<sub>3</sub>), nickel oxide (NiO), and iron sulphates (FeSO<sub>4</sub>, Fe<sub>2</sub>(SO<sub>4</sub>)<sub>3</sub>). The proportions of the phases present in the surface layer are inferred to be a consequence of both the strength of the oxidant employed, and the thermodynamic stability of the phases, as can be illustrated using partial pressure and Eh/pH diagrams. A sequence of oxidation is proposed, accounting for the sub-surface enrichment in violarite, and the development of the oxidized surface, which is inferred to have a major affect on the rates of oxidation.

**KEYWORDS:** pentlandite, violarite, sulphides, surface, XPS, AES, Mössbauer, spectroscopy.

## Introduction

PENTLANDITE, (Fe, Ni)<sub>9</sub>S<sub>8</sub>, is the major source of the world's supplies of nickel (Ramdohr, 1980; Craig and Vaughan, 1981), and for this reason, the alteration (in particular the oxidation) of the mineral, both in ore deposits and during the extraction process, is important with regard to the nickel yield from the ore. This investigation has provided information on the chemistry of pentlandite surfaces that may be applicable to the separation of pentlandite, since the surface compositions are important in respect to the extraction efficiency and are, therefore, of commercial interest.

The nature and mechanisms of supergene alte-

ration of pentlandite can also be studied by a characterization of the altered pentlandite surfaces, and the iron-nickel compounds present in natural ore assemblages as a result of the oxidation of pentlandite can be inferred. Previous investigations concerning the alteration of iron-nickel ore deposits (e.g. Nickel *et al.*, 1974; Thornber, 1975; Thornber and Wildman, 1979) are important with respect to this study and the interpretation of the surface alteration of pentlandite.

## Surface preparation

In order to avoid any possible effects of minor contaminant elements in the sample on the rates

Table 1. Final reflectance (R%) values measured for pentlandite oxidised in different media, relative to a WTiC standard.

Oxidant	IMA/COM standard wavelengths			
	470nm	546nm	589nm	650nm
Unoxidised	40	44	49	52
Air (low T furnace; 150°C)	29	37	41	44
Steam	28	36	40	44
Ammonium hydroxide	27	30	34	36
Sulphuric acid	24	28	32	35
Hydrogen peroxide	13	14	15	16
Electrochemical (0.8V in water)	13	14	15	15

and products of oxidation, synthetic pentlandite was used in this study. The pentlandite was synthesized by a direct combination of the elements to produce a phase containing equal proportions of iron and nickel,  $\text{Fe}_{4.5}\text{Ni}_{4.5}\text{S}_8$ . The mineral was produced using an evacuated silica tube synthesis (Scott, 1976) with primary homogenization at 150°C, followed by several weeks of homogenization at 600°C, below the maximum thermal stability of pentlandite at 610°C (Kullerud, 1963). Subsequent examination in polished section indicated the presence of a homogeneous pentlandite, and X-ray diffraction and electron microprobe analyses showed the average phase composition to be concordant with the initial synthesis composition. When examined in polished section the phase did not exhibit any surface cracking that might have been expected as a consequence of quenching.

The sample consisted of grains in random orientation, which is advantageous since the surface alteration may be affected by crystallographic orientation, even in a cubic mineral such as pentlandite. Thus, the materials analysed give an average composition for the pentlandite surfaces.

Pentlandite is unstable and oxidizes to a small extent in air and fairly rapidly in water. To enhance the effects of oxidation and to exemplify the processes of alteration occurring both in nature and during extraction, the synthetic pentlandite surfaces were oxidized by various substances in aqueous media under various Eh and pH conditions, and in air whilst heating at relatively low temperatures. The oxidant strengths and exposure times were based on unpublished work by the first author on the surface alteration of pyrite, pyrrhotine and chalcopyrite. The oxidants used were: (1) electrochemical under a potential of 0.8 V in water; (2) 3 M sulphuric acid for 30

minutes; (3) steam for 2 hours; (4) air (furnace at 150°C); (5) 10 M ammonium hydroxide for 30 minutes; (6) 25 vol. hydrogen peroxide for 20 minutes.

### Optical properties

Preliminary examination was undertaken using quantitative reflectance measurements. These were carried out using a Reichert reflex spectral microphotometer with a WTiC standard, as approved by the Commission on Ore Microscopy of the International Mineralogical Association. The technique of reflectance measurement, used as an indicator of the degree of oxidation, is employed here with caution, since the changes in reflectance observed will be affected by the character of the oxidized phases formed on the surface, the degree of scattering of the light by the oxidized layer, and the extent to which the subsurface reflects light. Nevertheless, these problems considered, the reflectance measurements of highly oxidized pentlandite surfaces yielded final reflectance values that were consistently proportional to the depth of oxidation. Table 1 shows reflectance measurements at the COM standard wavelengths of 470, 546, 589 and 650 nm, for unoxidized and oxidized pentlandite surfaces. The reflectance values may be used as an indication of the extent of alteration at the surface, although in the light of spectroscopic examination and chemical characterization, discussed below, the reflectance changes appear to be controlled by both the actual phases developed at the surfaces, and cracking of the surface during oxidation. Processes that lead to the cracking of the surface as a result of oxidation are discussed later.

### Auger electron spectroscopy

Auger electron spectroscopy (AES) was used to provide elemental surface compositions to approximately a 10 Å depth of analysis. The technique, and its applications to mineralogy have been discussed by Urch (1985) and Vaughan and Tossell (1986).

AES involves the detection of the Auger electrons that are excited in a secondary electron process. The Auger process involves the displacement of a core-level electron after bombardment by an incident electron. This results in a singly-ionized excited state, which relaxes when an electron from an outer orbital fills the vacancy in the core with the associated photoemission of a quantized Auger electron, leaving the element in a doubly-ionized state.

In this investigation, the Auger data were recorded using a Kratos XSAM 800 XPS/Auger spectrometer. The spectra were obtained in differentiated form after a primary electron-beam excitation of 3 keV. Depth profiling of the surface was obtained by combining AES with argon ion sputtering, (i.e. the mechanical erosion of the surface using argon ions, also known as 'etching'), producing an elemental profile with depth. The sputtering was undertaken using a Kratos Mini-beam 1 ion gun with a 5 keV voltage and  $1 \mu\text{Acm}^{-2}$  sample current, producing an estimated sputter rate of  $1 \text{ \AA min}^{-1}$ .

Fig. 1 shows an Auger/sputter graph for pentlandite oxidized by steam. This graph shows elemental compositions that are typical of the oxidized pentlandite surfaces investigated. These indicate a decrease in oxygen into the surface that is related inversely to an increase in sulphur. A major feature in these profiles is the presence, in all of the pentlandite surfaces studied, of an increase in the concentration of nickel with respect to iron below the immediate surface. This enrichment of nickel in the subsurface, and reasons for its development, are substantiated and explained in more detail in the following sections.

### X-ray photoelectron spectroscopy (XPS)

X-ray photoelectron spectra were also recorded using a Kratos XSAM 800 XPS/Auger spectrometer, using Mg-K $\alpha$  X-rays as the exciting radiation. XPS is important in the study of both altered and unaltered surfaces due to its excellent surface sensitivity with a penetration depth of approximately 10–15 Å. Thus, a surface layer of <15 Å can be analysed. The main use of XPS is in the determination of the chemical state of species in the altered surfaces.

The X-ray photoelectron effect involves the

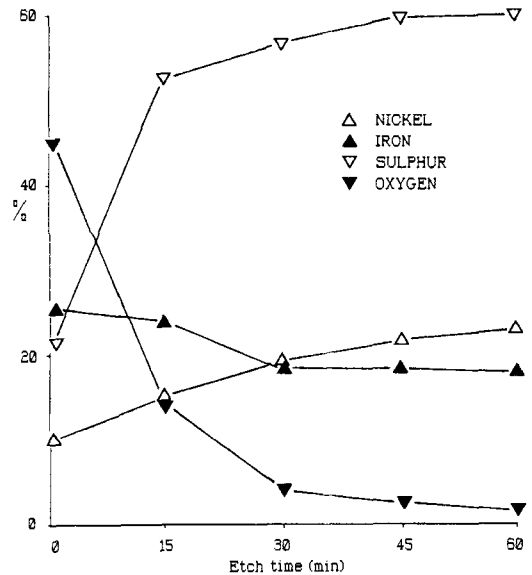


FIG. 1. Major element percentages derived from AES data with respect to etching. Estimated etch rate of  $1 \text{ \AA min}^{-1}$ , thus the lower scale is also an indication of the etch depth in Å.

ejection of core and valence electrons as a result of X-ray bombardment with, for example, Mg-K $\alpha$  X-radiation. The core and valence electrons are emitted with quantized kinetic energies, and these kinetic energies can be used to calculate the binding energies of electrons at particular energy levels. The binding energy variation between compounds for electrons from the same energy level can be used to distinguish between chemical phases in the analysed surface (Briggs and Seah, 1980). The mineralogical applications of XPS have been discussed by Urch (1985). The use of argon-ion sputtering (etching) to analyse chemical surfaces with depth, by combination with XPS, is not practicable due to the chemical reduction of surface components after sputtering, as discussed by Tsang *et al.* (1979).

The spectra obtained in this investigation were fitted using a non-linear least-squares fitting procedure. New data for selected energy levels in pentlandite are proposed, and previous data for peak positions and linewidths are included in Table 2. This table also includes data for the iron oxides and hydroxides (after McIntyre and Zetaruk, 1977; Harvey and Linton, 1981; Mills and Sullivan, 1983), sulphates (after Frost *et al.*, 1974; Limouzin-Maire, 1981) and nickel oxides (after McIntyre and Cook, 1975).

New data for the pentlandite Fe  $2p^{3/2}$  and Ni  $2p^{3/2}$  binding energies of 707.3 eV and 853.0 eV,

Table 2. X-ray photoelectron data: The binding energies (B.E.) and peak widths for relevant energy levels.

Compound	B.E. (eV)	Linewidth (eV)	Compound	B.E. (eV)	Linewidth (eV)
	<u>Fe 2p 3/2</u>			<u>O 1s</u>	
(Fe,Ni) <sub>9</sub> S <sub>8</sub>	707.3	0.9	Fe <sub>1-x</sub> O	530.0	0.7
FeNi <sub>2</sub> S <sub>4</sub>	708.4	0.9	Fe <sub>3</sub> O <sub>4</sub> (2+)	530.0	0.7
Fe <sub>1-x</sub> O	709.5	1.3	Fe <sub>3</sub> O <sub>4</sub> (3+)	531.4	1.1
Fe <sub>3</sub> O <sub>4</sub> (2+)	709.5	1.3	Fe <sub>2</sub> O <sub>3</sub>	531.4	1.1
Fe <sub>3</sub> O <sub>4</sub> (3+)	710.8	1.5	FeOOH (O)	530.0	0.7
Fe <sub>2</sub> O <sub>3</sub>	711.0	1.5	FeOOH (OH)	531.4	1.1
FeOOH	711.0	1.5	Fe(OH) <sub>3</sub>	531.4	1.1
Fe(OH) <sub>3</sub>	711.0	1.5	FeSO <sub>4</sub>	532.6	1.3
FeSO <sub>4</sub>	712.3	1.8	Fe <sub>2</sub> (SO <sub>4</sub> ) <sub>3</sub>	532.9	1.3
Fe <sub>2</sub> (SO <sub>4</sub> ) <sub>3</sub>	714.6	1.8	NiO	529.6	0.7
Fe <sup>2+</sup>	709.8	1.4	NiSO <sub>4</sub>	532.0	1.3
Fe <sup>3+</sup>	711.0	1.6		<u>S 2p</u>	
	<u>Ni 2p 3/2</u>		sulphides	161.2	0.9
(Fe,Ni) <sub>9</sub> S <sub>8</sub>	853.0	0.9	sulphur	162.5	1.2
FeNi <sub>2</sub> S <sub>4</sub>	853.2	0.9	FeSO <sub>3</sub>	165 - 6	1.4
NiO	854.0	1.1	FeSO <sub>4</sub>	168.0	1.4
NiSO <sub>4</sub>	858.0	1.8	Fe <sub>2</sub> (SO <sub>4</sub> ) <sub>3</sub>	168.2	1.4

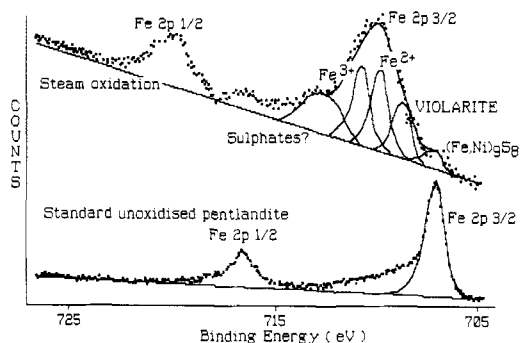


Fig. 2. Fe  $2p^{3/2}$  X-ray photoelectron spectra showing a pentlandite oxidized by steam in comparison to a spectrum for unoxidized pentlandite.

respectively, are proposed from the fitting of peaks to the unaltered pentlandite spectra. Similarly, a peak position of 161.2 eV was fitted for the pentlandite sulphur  $2p$  energy level.

The nickel  $2p^{3/2}$  energy level was also studied, and most of the spectra indicate a single peak for the sulphide in the unoxidized surface, broadening slightly after oxidation, and the develop-

ment of a second peak correlating with the presence of nickel oxide after oxidation in a furnace and by electrochemical methods. The nickel spectra indicate that nickel sulphate formation did not occur with any oxidant, which could be due in part to the high solubility of nickel sulphate, although evidence would be expected for its presence. Compared to the other analysed elements, there is a depletion of nickel-bearing alteration products in the surface.

The Fe  $2p$  spectra of altered surfaces are more complex. Fig. 2 shows an unaltered pentlandite spectrum and a pentlandite surface after oxidation by steam. In contrast to the nickel spectra, the Fe  $2p$  spectra indicate the formation of several iron compounds. The binding energies observed are consistent with a range of iron(II) and (III) oxides and hydroxides, with associated oxysulphates. Data for the iron oxides and hydroxide peak positions are extensive, but the overlapping of peaks as indicated in Table 2 makes it more expedient to fit the peaks in terms of the iron(II) and (III) oxidation states, rather than specific oxides and hydroxides. A problem arises in the determination of the sulphate peak area because, although the peak area has been defined pre-

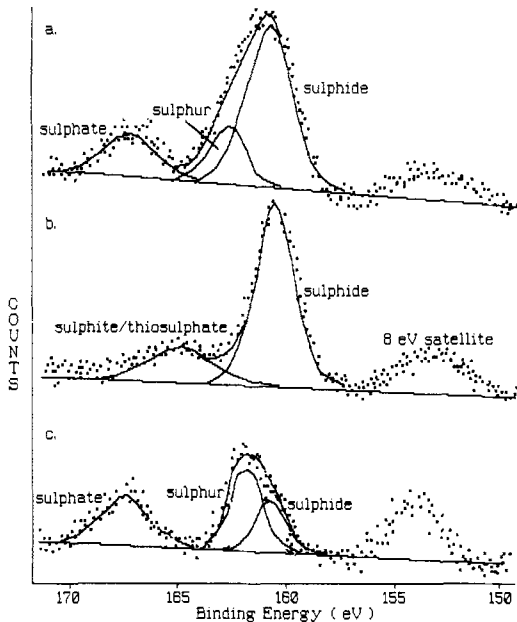


Fig. 3. Sulphur  $2p$  X-ray photoelectron spectra obtained for pentlandite oxidized by: (a) sulphuric acid, (b) steam, and (c) hydrogen peroxide.

viously in work by Frost *et al.* (1974) and Limouzin-Maire (1981), the spectra in this region, and to a lesser extent lower binding energies, are affected by shake-up lines from compounds with lower energies. Shake-up lines are prominent satellites caused, in this case, by the paramagnetic state of the Fe(II) and Fe(III) in the surface. This error in determining the peak area due to the sulphate is overcome by using the value obtained from the fitted sulphur  $2p$  spectra.

During fitting of the iron  $2p$  spectra, it was evident that there was a contribution to the spectrum from a compound with a binding energy slightly greater than that of pentlandite. In most of the surfaces studied a considerable contribution from sulphides to the sulphur  $2p$  spectra, as discussed later, was detected. This suggests, in combination with the minimal pentlandite Fe  $2p^{3/2}$  contribution, that a second sulphide is present.

Previous mineralogical studies of pentlandite (Nickel *et al.*, 1974; Thornber, 1975; Thornber and Wildman, 1979) have indicated that the secondary sulphide is most likely to be violarite. Analyses of a synthetic violarite, of composition  $\text{FeNi}_2\text{S}_4$ , provided new values of 708.4 eV for the Fe  $2p^{3/2}$ , 853.2 eV for the Ni  $2p^{3/2}$ , and a sulphur  $2p$  value the same as that measured for pentlandite. Fitting the Fe  $2p^{3/2}$  spectra with the violarite contribution produced accurate fits to the mea-

sured spectra. Other possible secondary sulphides were considered, but the binding energies were not consistent with the oxidized pentlandite spectra.

In assessing the alteration of sulphide surfaces, much information can be gained from a study of the mobile elements, sulphur and oxygen, and their compounds. The sulphur  $2p$  energy level is important also, with respect to the wide energy range, of about 7 eV, between the compounds present, allowing good resolution of the peak fitting. Fig. 3 illustrates this resolution, and indicates that the sulphur species present at the surface can vary considerably. The presence of sulphide in most surfaces is evident, confirming, with the Fe  $2p^{3/2}$  spectra, the presence of violarite.

Oxygen  $1s$  spectra for four oxidized surfaces are shown in Fig. 4 and can be used to demonstrate the formation of nickel oxide and to determine the relative amounts of sulphate with respect to iron and nickel oxides. The range of binding energies present in the oxygen  $1s$  spectra is small, from 529.6 eV for nickel oxide to 532.9 eV for ferric sulphate, complicating the resolution of the spectra. In Fig. 4, an attempt at resolving the peaks present, in simplified form, has been made.

These spectra show a limited presence of nickel oxide, after furnace and electrochemical oxidation only. It was also evident that, although sulphates were consistently present in all surfaces analysed, the occurrence of iron oxides and hydroxides was variable.

An assessment of the surface compositions, as derived from X-ray photoelectron spectra is included in Table 3.

#### Conversion electron Mössbauer spectroscopy

Another important source of information on surface chemistry is given by conversion electron Mössbauer spectroscopy (CEMS). CEMS is a surface (approximately 1000 Å penetration) technique that detects conversion electrons emitted from the surface as a result of an instantaneous relaxation process after gamma absorption. An overview of the Mössbauer effect can be obtained in Bancroft (1973) and Wertheim (1964), with specific mineralogical applications described by Maddock (1985).

Study by CEMS of the unoxidized pentlandite gave a spectrum with a quadrupole doublet. Fitted parameters for the pentlandite were  $0.333 \text{ mms}^{-1}$  for the isomer shift and  $0.336 \text{ mms}^{-1}$  for the quadrupole splitting, indicating iron predominantly in tetrahedral sites. Previous work (Vaughan and Ridout, 1971) indicates that pentlandite can have iron present in both tetrahedral and octahedral

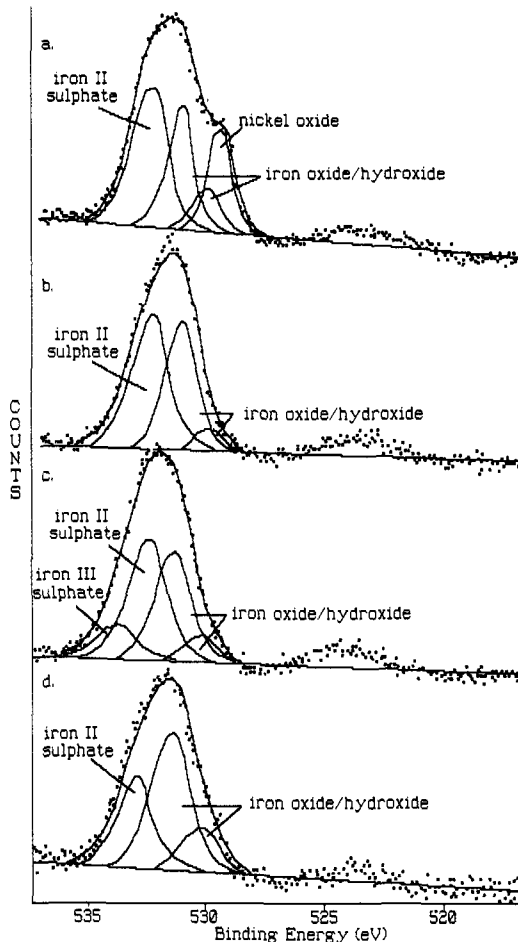


Fig. 4. Oxygen 1s X-ray photoelectron spectra for pentlandite surfaces obtained following oxidation by: (a) air in a furnace at 150°C, (b) sulphuric acid, (c) hydrogen peroxide, and (d) ammonium hydroxide.

sites. However, as reported by Knop *et al.* (1970), the iron diffuses into tetrahedral sites during annealing, as may be the case with the synthetic pentlandite investigated.

After oxidation, with any of the oxidants used, a second quadrupole doublet is observed, as shown in Fig. 5. Fitted parameters for the second doublet, are  $0.320 \text{ mms}^{-1}$  for the isomer shift and  $0.610 \text{ mms}^{-1}$  for the quadrupole splitting, in agreement with previous work on violarite and indicating iron in octahedral sites (Vaughan and Craig, 1985). The other surface oxidation products, as identified in the studies by XPS, were not present in quantities sufficient to be detected by CEMS.

### Structural transformation

The rapid formation of violarite in the pentlandite subsurface is promoted by the instability of pentlandite, and more importantly, by the similarity between the crystal structures. Misra and Fleet (1974) investigated the pentlandite transformation to violarite in ore samples from nickel deposits and concluded that the alteration could be caused by the removal of excess metal atoms, largely iron, and the formation of violarite around the similar, face-centred cubic, sulphur atom sub-structure.

The transformation involves a reduction in cell size from the pentlandite ( $10.06 \text{ \AA}$  cell edge) to the violarite ( $9.46 \text{ \AA}$  cell edge), an overall volume reduction of 17%. A consequence of the structural transformation and volume reduction was the formation of shrinkage cracks on the surface. A typically altered, and cracked surface is shown in the photomicrograph in Fig. 6, which also indicates the formation of oxidant layers developed over what is essentially a cracked sub-surface.

### Interpretation of the chemistry of oxidized surfaces

The spectroscopic methods used enable the surface elemental and compound compositions to be estimated. These indicate that after oxidation there is a depletion in iron at depth, leading to the formation of violarite. However, the oxidized layer, consisting of sulphates, oxides and hydroxides is only of approximately  $10 \text{ \AA}$  depth. There is a variation in composition of the oxidized layer, and to a lesser extent, the sub-surface, that depends on the oxidant used.

Prominent on all of the surfaces is the formation of iron sulphates and iron oxides/hydroxides, with a ratio of  $\text{Fe}^{2+}$  to  $\text{Fe}^{3+}$  that decreases with the effective strength of the oxidant. In general, the principal  $\text{Fe}^{2+}$ -bearing compound is probably magnetite ( $\text{Fe}_3\text{O}_4$ ). The  $\text{Fe}^{3+}$  occurs in a number of forms, with the potential formation of hematite ( $\text{Fe}_2\text{O}_3$ ) and oxy-hydroxides ( $\text{FeOOH}$ ), with an  $\text{Fe}^{3+}$  component of magnetite present. In aqueous oxidants, however, the predominant phase is expected to be  $\text{FeOOH}$ .

A major difference between the surfaces studied was the variability in the proportion of elemental sulphur detected in the surface layers, which may be a result of the rapid dissolution of iron and nickel ions from the surface. In considering the nature of the transformation of pentlandite to violarite, occurring without a sulphur loss, the formation of elemental sulphur and sulphates indicate that the pentlandite is either alter-

Table 3. Estimated percentages of phases present in the 10–15 Å surface layer of oxidised pentlandite, derived from X-ray photoelectron data.

Compound	Oxidants					
	H <sub>2</sub> O	H <sub>2</sub> SO <sub>4</sub>	steam	O <sub>2</sub> /air	NH <sub>4</sub> OH	H <sub>2</sub> O <sub>2</sub>
	0.8 V	3M	2hr	150°C	10M	25 vol
	20 min	30 min		3 days	30 min	20 min
FeSO <sub>4</sub> /Fe <sub>2</sub> (SO <sub>4</sub> ) <sub>3</sub>	25	27	28	30	28	32
NiO	9	-	-	12	-	-
Fe <sup>3+</sup> oxides/	14	16	25	25	40	20
Fe <sup>2+</sup> hydroxides	16	7	23	15	7	12
Sulphur	-	23	-	6	14	27
FeNi <sub>2</sub> S <sub>4</sub>	24	21	19	11	9	9
(Fe,Ni) <sub>9</sub> S <sub>8</sub>	12	6	5	1	2	-

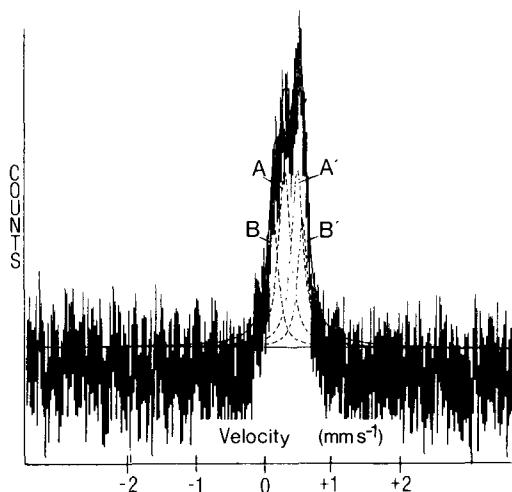


FIG. 5. Conversion electron Mössbauer spectrum for pentlandite oxidized by hydrogen peroxide. The quadrupole doublet AA' corresponds to iron in pentlandite tetrahedral sites. After oxidation the quadrupole doublet BB' is fitted corresponding to octahedral sites in violarite.

ing directly, or ultimately via violarite, to oxygen-containing phases.

Nickel compounds are depleted in the oxidized surface, being detected in only the electrochemically and furnace oxidized samples. This may be as a result of dissolution rates, where the nickel compounds are formed in the surface and then dissolved, whereas in the furnace there was no form of dissolution. The presence of nickel oxide in the electrochemically oxidized surfaces is prob-

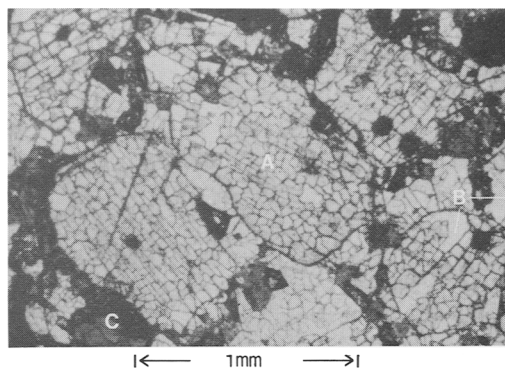


FIG. 6. Photomicrograph showing electrochemically oxidized pentlandite with evidence of shrinkage cracks (A). Overlaying the cracked sub-surface, thin oxidation layers are evident (B). The granular nature of the synthetic pentlandite is evident from the partially infilled holes (C).

ably due to an oxidation rate that supersedes the rate of dissolution. In considering the nature of the nickel in the surface, it has been inferred that the nickel is present as either sulphides or nickel oxide. The nickel-containing oxides developed after oxidation may also be interpreted as either amorphous iron–nickel oxides, which could be indicated from the amorphous nature of the oxidized surfaces as studied by scanning electron microscopy, or present as a specific iron–nickel oxide, for example trevorite, NiFe<sub>2</sub>O<sub>4</sub>. Since the spectroscopic methods used cannot differentiate between the phases, the oxide of nickel detected is reported as NiO.

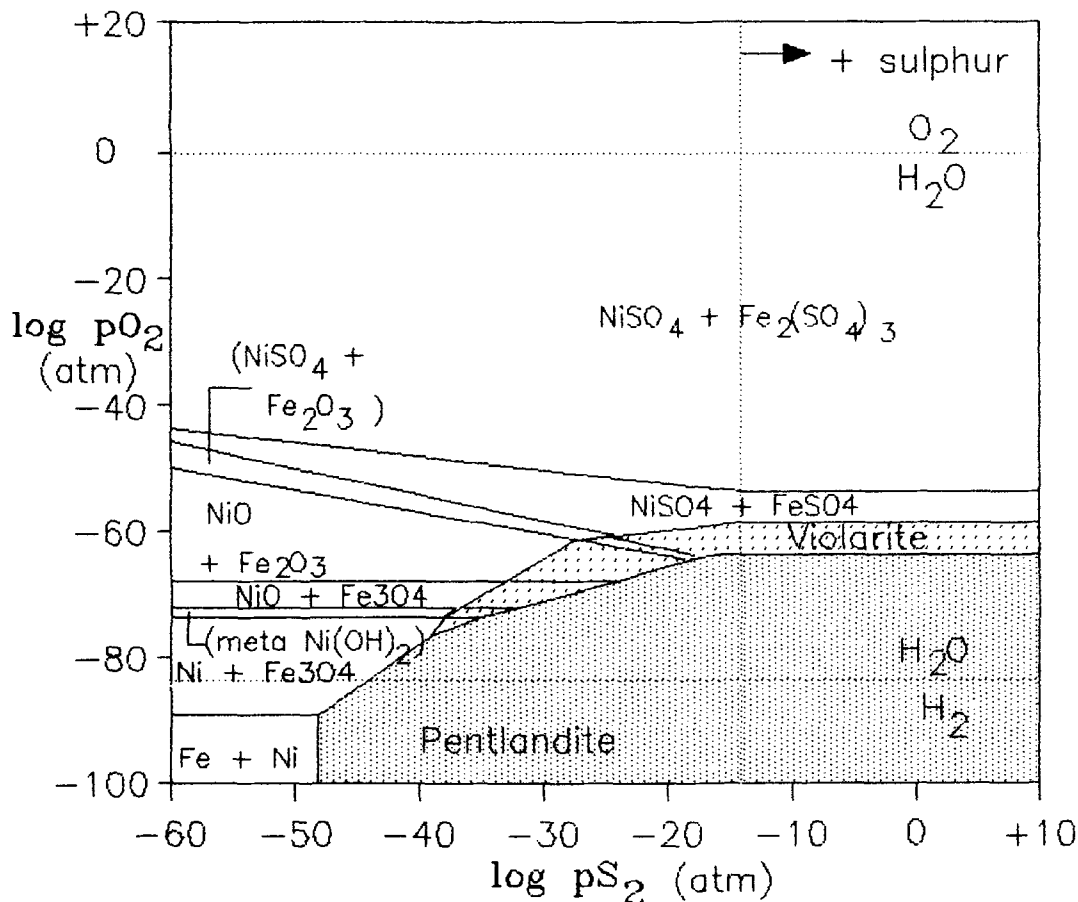


Fig. 7.  $\log p_{O_2}$  versus  $\log p_{S_2}$  partial pressure diagram for altered pentlandite, constructed with respect to violarite. (Estimated free energies of formation for pentlandite and violarite, of  $-780$  and  $-330$   $\text{kJ mol}^{-1}$ , respectively).

Considering the stability of pentlandite with respect to violarite and the oxidation products, in terms of partial-pressure (Fig. 7) and Eh/pH diagrams (Fig. 8), the surfaces are consistent, for the most part, with the thermochemically determined products of oxidation. In the partial-pressure diagram, the relative stability of violarite to pentlandite is indicated, and also the possibility that any violarite forming in the immediate surface may oxidize further. The potential for nickel sulphate formation is defined by this diagram, and when used in conjunction with the Eh/pH diagram, indicates that it will not form on the pentlandite surfaces in aqueous oxidants because of the formation of aqueous nickel ions. In the partial pressure and Eh/pH diagrams the iron(III) species is  $\text{Fe}_2\text{O}_3$ , as the long-term stable iron(III) phase, but  $\text{FeOOH}$  would be expected to form

as the more stable initial iron(III) phase in the aqueous oxidants.

### Summary

The oxidation of pentlandite can be summarized as follows. Primary alteration of the surfaces proceeds rapidly with the oxidized surface developing iron compounds at a faster rate than nickel compounds. This phenomenon is shown in the analyses of furnace oxidized pentlandite, where no dissolution process can take place. Where dissolution is a factor, the nickel compounds are further depleted. Variations in the surface compositions are affected by the thermochemical stability of the oxidation products in the oxidation media.

After initial rapid oxidation, an iron-rich oxi-

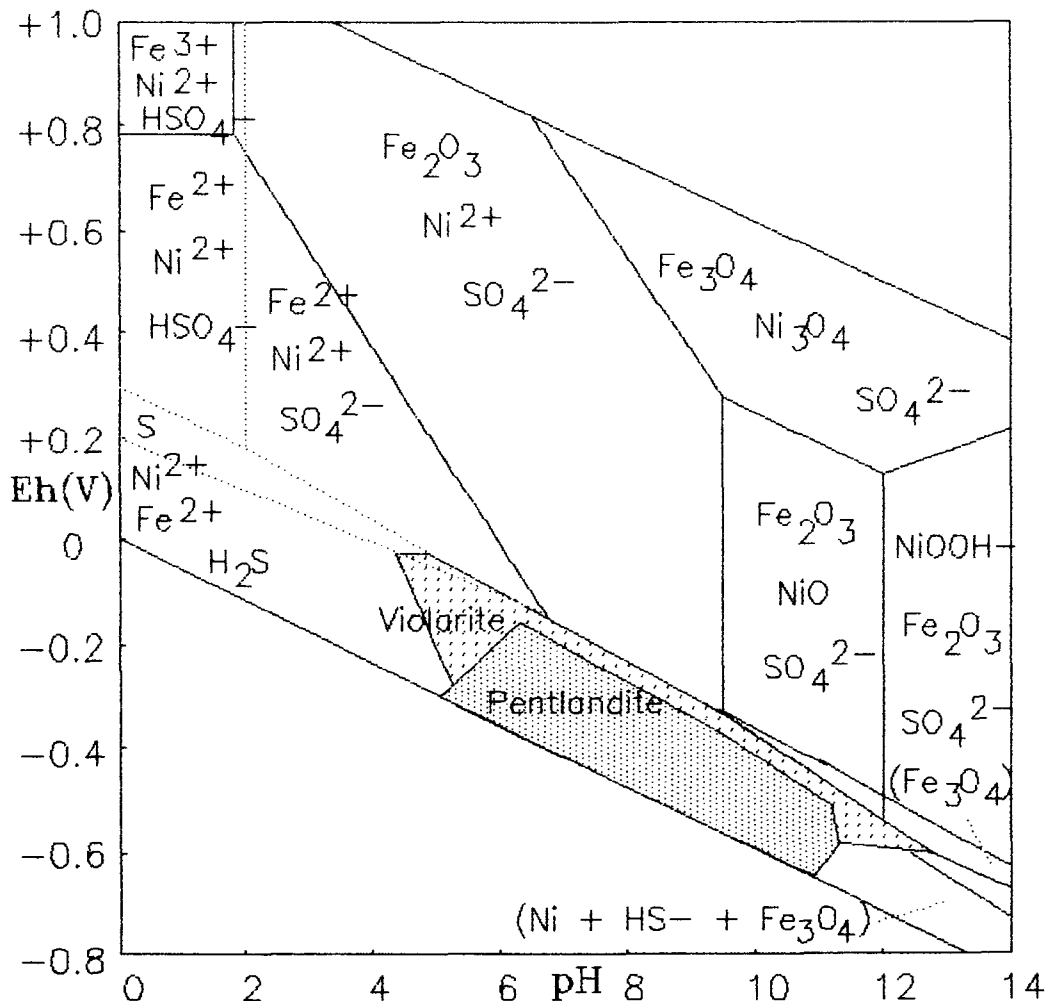


Fig. 8. Eh/pH diagram for the alteration of pentlandite, indicating the preferential stability of violarite. (Estimated free energies of formation for pentlandite and violarite, of  $-780$  and  $-330$   $\text{kJ mol}^{-1}$ , respectively).

dized layer is developed. This layer may act as an inert barrier preventing further rapid oxidation into the surface. Further oxidation would then proceed as a result of diffusion through the oxidized layer, resulting in further preferential iron loss. Consequently, the iron-deficient sub-surface sulphide transforms from pentlandite to violarite. This is comparable with Buckley and Woods (1984) model for the sub-surface copper sulphide enrichment of chalcopyrite.

#### Acknowledgements

The authors would like to thank Mr A. Abbot, and the Department of Electrical and Electronic Engineering and Applied Physics, Aston University, for help in

obtaining the XPS and Auger spectra. Financial support from NATO (Grant 833/83 to D. J. Vaughan and J. Tossell) is gratefully acknowledged, as is the provision of a Studentship by the University of Aston to S. Richardson.

#### References

- Bancroft, G. M. (1973) *Mössbauer spectroscopy: An introduction for inorganic chemists and geochemists*. McGraw-Hill.
- Briggs, D. and Seah, M. P. (1980) *Practical surface analysis by Auger and X-ray photoelectron spectroscopy*. Wiley.
- Buckley, A. N. and Woods, R. (1984) An X-ray photoelectron spectroscopic study of the oxidation of chalcopyrite. *Aust. J. Chem.* **37**, 2403–13.

- Craig, J. R. and Vaughan, D. J. (1981) *Ore microscopy and ore petrography*. Wiley.
- Frost, D. C., Leeder, W. R. and Tapping, R. L. (1974) X-ray photoelectron spectroscopic study of coal. *Fuel* **53**, 206–11.
- Harvey, D. T. and Linton, R. W. (1981) Chemical characterisation of hydrous ferric oxides by X-ray photoelectron spectroscopy. *Anal. Chem.* **53**, 1684–8.
- Knop, O., Huang, C.-H. and Woodhams, F. W. D. (1970) Chalcogenides of the transition elements. VII. A Mössbauer study of pentlandite. *Am. Mineral.* **55**, 1115–30.
- Kullerud, G. (1963) Thermal stability of pentlandite. *Can. Mineral.* **7**, 353–66.
- Limouzin-Maire, Y. (1981) Etude par spectroscopie ESCA de sulfures et sulfates de manganèse, fer, cobalt, nickel, cuivre et zinc. *Bull. Chim. Soc. (Fra) Pt. 1*, 340–3.
- Maddock, A. G. (1985) Mössbauer spectroscopy in mineral chemistry. In *Chemical bonding and spectroscopy in mineral chemistry*. (Berry F. J. and Vaughan D. J., eds.) Chapman and Hall.
- McIntyre, N. S. and Zetaruk, D. G. (1977) X-ray photoelectron spectroscopic studies of iron oxides. *Anal. Chem.* **49**, 1521–9.
- and Cook, M. G. (1975) XPS studies on some oxides and hydroxides of cobalt, nickel and copper. *Ibid.* **49**, 2208–15.
- Mills, P. and Sullivan, J. (1983) An XPS study of the bonding of core level electrons in iron oxides. *J. Phys. D: Appl. Phys.* **16**, 723–32.
- Misra, K. C. and Fleet, M. E. (1974) Chemical composition and stability of violarite. *Econ. Geol.* **69**, 391–403.
- Nickel, E. H., Ross, J. R. and Thornber, M. R. (1974) The supergene alteration of pyrrhotite-pentlandite ore at Kambalda, Western Australia. *Ibid.* **69**, 93–107.
- Ramdohr, P. (1980) *The ore minerals and their intergrowths* (2nd ed.) Pergamon Press.
- Scott, S. D. (1976) Experimental methods in sulphide synthesis. Reviews in Mineralogy **1**, *Sulphide mineralogy* (Ribbe, P. H., ed. Min. Soc. Am.)
- Thornber, M. R. (1975) Supergene alteration of sulphides, 1. A chemical model based on massive nickel sulphide deposits at Kambalda, Western Australia. *Chem. Geol.* **15**, 1–14.
- and Wildman, J. E. (1979) Supergene alteration of sulphides, 4. Laboratory study of the weathering of nickel ores. *Ibid.* **24**, 97–110.
- Tsang, T., Coyle, G. J., Adler, I. and Yin, L. (1979) XPS studies of ion bombardment damage in iron-sulphur compounds. *J. Electron Spectroscopy and related phenomena* **16**, 389.
- Urch, D. S. (1985) X-ray spectroscopy and chemical bonding in minerals. In *Chemical bonding and spectroscopy in mineral chemistry*. (Berry, F. J. and Vaughan, D. J., eds.) Chapman and Hall.
- Vaughan, D. J. and Craig, J. R. (1985) The crystal chemistry of iron-nickel thiospinels. *Am. Mineral.* **70**, 1036–43.
- and Ridout, M. S. (1971) Mössbauer studies of some sulphide minerals. *J. Inorg. Nucl. Chem.* **33**, 741–6.
- and Tossell, J. A. (1986) Interpretation of the Auger electron spectra of sulfide minerals. *Phys. Chem. Mineral.* **13**, 347–50.
- Wertheim, G. K. (1964) *Mössbauer effect: Principles and applications*. Academic Press.

[Manuscript received 17 March 1988]